On the Quenching of $\mathrm{MLCT}_{\mathrm{Re}\rightarrow\mathrm{bpy}}$ Luminescence by Cu(II) Species in Re(I) Polymer Micelles

Ezequiel Wolcan,*,[†] José L. Alessandrini,[‡] and Mario R. Féliz*,[§]

INIFTA, Facultad de Ciencias Exactas, Universidad Nacional de La Plata,
Casilla de Correo 16, Sucursal 4, (1900) La Plata, República Argentina

Received: July 8, 2005; In Final Form: September 22, 2005

Transmission electron microscopy (TEM) and dynamic light scattering (DLS) studies on acetonitrile solutions of the polymer $\{[(vpy)_2\text{-}vpyRe(CO)_3bpy]\ CF_3SO_3\}_{200}$ demonstrated that the Re(I) polymer molecules aggregate to form spherical micelles of radius $R = 156$ nm. Coordination of Cu(II) species to the Re (I) polymer causes a decrease in the micelle radius and a distortion from the spherical shape. Besides, the coordination of Cu(II) species to the $\{[(vpy)_2\text{-}vpyRe(CO)_3bpy]\ CF_3SO_3\}_{200}$ polymer produces the quenching of the metal to ligand charge transfer (MLCT) excited state by energy transfer processes that are more efficient than those in the quenching of the monomer $pyRe(CO)_3bpy^+$ luminescence by Cu(II). Moreover, the kinetics of the quenching by Cu(II) do not follow a Stern−Volmer behavior. Conversely, the quenching of the MLCT luminescence of the Re(I) polymer by the sacrificial electron donor 2,2′,2″-nitrilotriethanol, TEOA, follows a Stern−Volmer kinetics. A comparison is made between the quenching by CuX_2 (X = Cl or CF_3SO_3) and TEOA.

Introduction

During the past three decades, numerous studies have been concerned with luminescent Re(I) tricarbonyl complexes coordinated to mono or bidentate azines. The accessible excited states, Re(I) to azine metal-to-ligand charge transfer (MLCT), ligand-to-ligand charge transfer (LLCT), and/or intraligand (IL) excited states, are generally involved with the observed luminescence at room temperature.[1−5] A rational design in the synthesis of the azine ligands was used to tune the photophysical and photochemical properties of the metal complexes in order to obtain photosensitizers that might be utilized in areas such as electron-transfer studies,[6] solar energy conversion,[7−9] and potential technical applications to catalysis.[10]

Another approach, however, involved the synthesis of compounds where the metal complex containing the chromophore unit was attached to an organic polymeric backbone. Much of the literature examples involve transition metal ions metalating poly(*p*-phenylenevinylene) polymers incorporating 2,2′-bipyridines,[11−13] polypyridil Ru(II) and/or Os(II) derivatized polystyrene,[14−24] and some multimetallic oligomeric complexes containing Ru(II) and Os(II) coordinated to 1,10-phenanthroline (phen).[25] However, little attention has been paid to Re(I) polymeric complexes. A previous work has shown marked differences between the photochemical and the photophysical properties of the monomer $pyRe(CO)_3(phen)^+$ and the related polymer $[(vpy)_2\text{-}vpyRe(CO)_3phen^+]_{n\sim200}$ (vpy= vinylpyridine, py= pyridine), revealing the presence of intrastrand electron and energy transfer processes.[26] A recent work by Schanze et al. dealt with the photophysics of π-conjugated Re(I) oligomers of aryleneethynylenes that contain the $(bpy)Re(CO)_3Cl$ chromophore (bpy = 2,2′-bipyridine).[27] Photophysical properties in those Re(I) compounds were dominated by the intense $\pi \rightarrow \pi^*$ transitions of the oligomeric aryleneethynylenes, with the exception of the shorter Re-oligomer of the series, where the MLCT was the lowest excited state.

We have previously investigated solvent and temperature effects on the photophysical properties of the polymer $\{[(vpy)_2\text{-}vpyRe(CO)_3bpy]CF_3SO_3\}_{n\sim200}$ and the related monomer $CF_3SO_3[pyRe(CO)_3bpy]$. Differences between the polymer and the monomer photophysical behavior were rationalized in terms of solvent and thermal effects on the transition between rigid rod and coil structures of the Re(I)−polymer.[28]

The formation of micelles has been reported in polystyrene-*block*-poly(4-vinylpyridine) (PS-*b*-PVP) functionalized with pendants $-Re(CO)_3(bpy)^+$ groups. Two PS-*b*-PVP− $Re(CO)_3(bpy)^+$ polymers with different Re(I) content exhibited the formation of rodlike and/or spherical micelles, as shown by transmission electron microscopy and light scattering experiments.[29, 30]

Coordination of Cu(II) ions to poly-4-vinylpyridine has been reported in the literature.[31−35] In this paper, we report the aggregation of single polymer molecules to form spherical micelles in acetonitrile solutions of the $\{[(vpy)_2\text{-}vpyRe(CO)_3bpy]\text{-}CF_3SO_3\}_{n\sim200}$ polymer and in the polymers formed after coordination of Cu(II) species to $\{[(vpy)_2\text{-}vpyRe(CO)_3bpy]CF_3SO_3\}_{n\sim200}$. We also explore the quenching of the Re(I) polymer's MLCT excited state by the coordination of CuX_2 (X = Cl or CF_3SO_3) to the free pyridines of the polymer backbone. A comparison is made between the quenching by CuX_2 and the quenching by the sacrificial electron donor TEOA.

Experimental Section

Materials. $CF_3SO_3[pyRe(CO)_3bpy]$ and the polymer $\{[(vpy)_2\text{-}vpyRe(CO)_3bpy]\ CF_3SO_3\}_{n\sim200}$ (Re−P4VP) were available from

---

* To whom correspondence should be addressed. Phone: 54-221 425 7430/425 7291. Fax: 54-221 425 4642. E-mail: ewolcan@inifta.unlp.edu.ar (E.W.); mfeliz@inifta.unlp.edu.ar (M.R.F.).

[†] Member of CONICET. Departamento de Química, Facultad de Ciencias Exactas, UNLP.

[‡] Member of CICPBA. Departamento de Física, Facultad de Ciencias Exactas, UNLP.

[§] Member of CICPBA. Departamento de Química, Facultad de Ciencias Exactas, UNLP.

10.1021/jp053758j CCC: $30.25

SCHEME 1

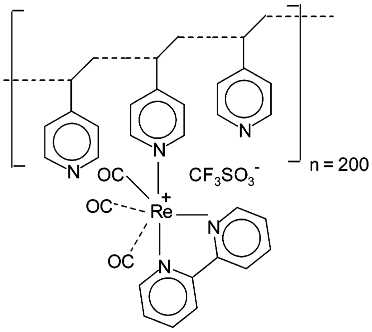

a previous work.[28] The polymer can be assigned the formal structure, Scheme 1, where pendants $-\mathrm{Re(CO)_3bpy}$ groups are randomly distributed along the strand of the polymer with an average of two uncoordinated 4-vinylpyridine groups for each one coordinated to a $-\mathrm{Re(CO)_3bpy}$ chromophore.

$\mathrm{CuCl_2{\cdot}2H_2O}$ (Riedel-de-Haën) was dried under vacuum at 80 °C until constant weight to obtain anhydrous $\mathrm{CuCl_2}$, which was then mantained in a dissecator. $\mathrm{Cu(CF_3SO_3)_2}$ was obtained by a displacement reaction between $\mathrm{CuCl_2{\cdot}2H_2O}$ and $\mathrm{AgCF_3SO_3}$ in acetonitrile after removing the precipitated AgCl by filtration. The acetonitrile solution containing $\mathrm{Cu(CF_3SO_3)_2}$ was rotoevaporated to dryness, and then the remaining solid was dried under vacuum at 80 °C until constant weight to obtain anhydrous $\mathrm{Cu(CF_3SO_3)_2}$. Acetonitrile (J. T. Baker) and TEOA (J. T. Baker) were reagent grade and were used without further purifications.

Light Scattering Intensity Measurements. The time correlation $G(q,t)$ of the light scattering intensity was measured at 90° with a goniometer ALV/CGS-5022F with Multiple Tau digital correlator ALV-5000/EPP covering a wide time range ($10^{-6}-10^{3}$ s). The light source was an helium/neon laser with a wavelength 633 nm operating at 22 mW. All of the measurements were carried out at room temperature.

Under homodyne conditions, valid for the present system, the measured $G(q,t)$ at a given wave vector $q = (4\pi n/\lambda)\sin(\theta/2)$ (n being the refractive index of the medium, λ is the wavelength in a vacuum and θ is the scattering angle) is related to the desired normalized electric field correlation function $g(q,t)$ by

$$G(q,t) = A_\infty[1 + f^*|\alpha\, g(q,t)|^2] \tag{1}$$

where f^* is an instrumental factor, α is the fraction of the total scattered intensity $I(q)$ arising from fluctuations in the optical polarizability with correlation times longer than about 10^{-6} s, and A_∞ is the baseline measured at long delay times.

The incident laser beam was polarized perpendicular to the scattering plane. $I(q)$ is the isotropic component of the light scattering intensity due to density and concentration fluctuations with the former being, in principle, much faster.

The characteristic relaxational parameters are extracted by carrying out the inverse Laplace transformation (ILT) of the measured $G(q,t)$ assuming a superposition of exponentials[36]

$$\left\{\frac{\left[\dfrac{G(q,t)}{A_\infty}\right] - 1}{f^*}\right\}^{1/2} = \alpha\, g(q,t) = \int_{-\infty}^{\infty} L(\ln\tau)\mathrm{e}^{-t/\tau}\, d(\ln\tau) \tag{2}$$

Static light scattering (SLS) measurements were performed at two scattering angles to get estimations of the radius of gyration through the dissymmetry method.[37]

TEM. Transmission electron micrographs were recorded on a JEOL 100 CX electron microscope at an electron acceleration voltage of 80 kV with a nominal point-to-point resolution of 3 Å. The photos were taken at an amplification of 20 000×.

Flash Fluorescence Procedures. Luminescence lifetime measurements were performed at room temperature by excitation with a Laseroptics nitrogen laser (7 ns fwhm and 2mJ/pulse at 337 nm). A modified 1P28 photomultiplier tube circuit with ca. 1 ns response time was used as the detector for the green emission dispersed through a monochromator. Decays typically represented the average of 10−30 pulses and were collected on a HP-54600B digital oscilloscope interfaced with a PC computer. Solutions for the photochemical work were deaerated with streams of ultrahigh-purity $\mathrm{N_2}$ before and during the irradiations.

Steady-State Irradiations. The luminescence of the Re(I) complexes was investigated in a Perkin-Elmer 50-B spectrofluorimeter interfaced to a microcomputer. The spectra were corrected for differences in instrumental response and light scattering. Solutions were deaerated with $\mathrm{O_2}$-free nitrogen in a gastight apparatus before recording the spectra.

General methods. UV−vis spectra were recorded on a Cary 3 spectrophotometer.

Results

Binding of Cu(II) to the Re(I)−Polymer. The addition of an acetonitrile solution of $\mathrm{CuX_2}$ (X = Cl or $\mathrm{CF_3SO_3}$) to an acetonitrile solution of the polymer Re−P4VP ([Re(I)] $\sim 8 \times 10^{-4}$ M, $[\mathrm{py}]_{\mathrm{uncoordinated}} \sim 1.5 \times 10^{-3}$M) produces a rapid coordination of the Cu(II) species to the uncoordinated pyridines of the Re−P4VP polymer. Indeed, after the mixing of the solutions there is an instantaneous change in the solution color from yellow to green, due to the appearance of a new absorption band. The coordination of the Cu(II) species to the Re(I) polyelectrolyte was followed by the UV−vis spectral changes of the weak ligand field d−d bands of Cu(II) in the range 500−900 nm, where the polymer Re−P4VP has no significant absorption. The addition of $\mathrm{CuCl_2}$ to the Re(I) polymer produces the growth of a new absorption band, centered at $\lambda_{\max} \sim 725$ nm, which is blue shifted respect to the d−d bands of the "free" $\mathrm{CuCl_2}$ ($\lambda_{\max} \sim 850$ nm). After the coordination of Cu(II) is complete, the solution spectrum maximum shifts from $\lambda_{\max} \sim 725$ to 850 nm due to the presence of increasing amounts of uncoordinated $\mathrm{CuCl_2}$ in the solution. From a linear fit analysis of the initial and final slopes of the plot $A_{725\ \mathrm{nm}}$ vs [Cu(II)] it could be calculated that the maximum amount of Cu(II) bound to the polymer was $[\mathrm{Cu(II)}]_{\mathrm{b,max}} = 6 \times 10^{-4}$ M, i.e., between one-half and one-third of the total initial free pyridine concentration. Similar spectral changes were observed after the addition of a solution of $\mathrm{Cu(CF_3SO_3)_2}$ to a solution of the polymer Re−P4VP in the same experimental conditions ([Re(I)] $\sim 8 \times 10^{-4}$ M, $[\mathrm{py}]_{\mathrm{uncoordinated}} \sim 1.5 \times 10^{-3}$M). The addition of $\mathrm{Cu(CF_3SO_3)_2}$ to the Re(I) polymer generates a new absorption band centered at $\lambda_{\max} \sim 610$ nm which is blue shifted respect to the d−d bands of the "free" $\mathrm{Cu(CF_3SO_3)_2}$ ($\lambda_{\max} \sim 750$ nm). After the saturation of the polymer with $\mathrm{Cu(CF_3SO_3)_2}$, there is a progressive shifting of the absorption maximum from 610 to 750 nm due to the presence of increasing amounts of uncoordinated $\mathrm{Cu(CF_3SO_3)_2}$ in the solution. From a linear fit analysis of the initial and final slopes of the plot $A_{600\ \mathrm{nm}}$ vs [Cu(II)] it could be calculated that the maximum amount of Cu(II) bound to the polymer was $[\mathrm{Cu(II)}]_{\mathrm{b,max}} = 4 \times 10^{-4}$ M, i.e., less than one-third of the total initial free pyridine concentration. It is worthy to note that the coordination of Cu(II) to the polymer

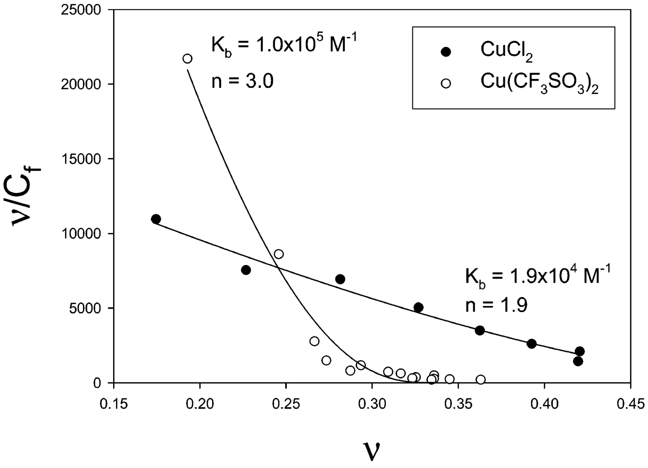

Figure 1. McGhee−von Hippel plot for the binding between Cu(II) species and $\{[(vpy)_2\text{-}vpyRe(CO)_3bpy]\ CF_3SO_3\}_{n\sim200}$. The solid lines represent the best fit of the experimental data according to eq 3.

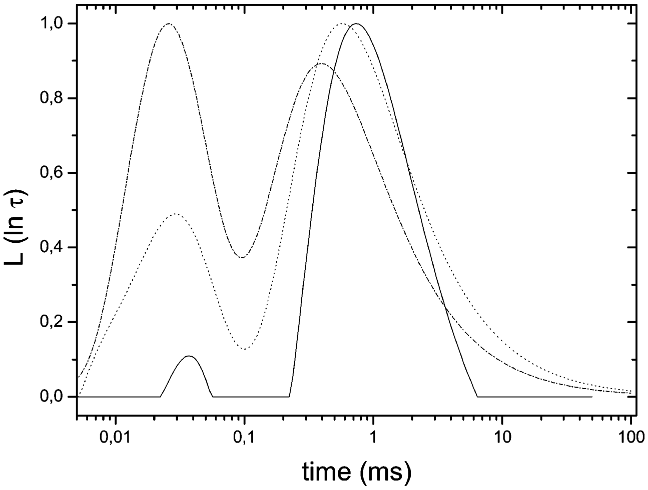

Figure 2. Representative relaxation time distribution L(ln τ) versus time at polymer concentrations 0.5 mg mL^{-1}. Full line: Re−P4VP polymer; dot−dash: Re−P4VP−CuCl$_2$ polymer; dot: Re−P4VP−Cu-(CF$_3$SO$_3$)$_2$ polymer.

Re−P4VP produces an increase in the extinction coefficient of the d−d transitions of the CuX$_2$ (X = Cl or CF$_3$SO$_3$). Quantitative treatment of UV−vis spectral changes allows the determination of the binding constants between Cu(II) and the pyridines in the Re(I) polyelectrolyte according to different theories.[38−39] We chose that of McGhee and von Hippel,[39] which describes random noncooperative binding to a lattice

$$\frac{\nu}{C_f} = K_b \frac{(1 - n\nu)^n}{[1 - (n - 1)\nu]^{n-1}} \tag{3}$$

where ν is the binding ratio C_b/[py], K_b is the binding constant, and n is the average size of a binding site (expressed in number of pyridines per Cu(II) species). To use this equation, the concentration of Cu(II) bound (C_b) and Cu(II) free (C_f) for each total concentration of Cu(II) ($C_T = C_b + C_f$) have to be determined. Therefore, C_b was calculated from the UV−vis absorption data as follows: for each total Cu(II) concentration, the difference $A_{polymer+Cu} - A_{Cu}$ must be proportional to C_b and eventually reaches a limiting value for $C_T \gg C_b$. From this we can obtain the ratio $C_b/C_{b,max}$ for each C_T. Finally, with the known values of $C_{b,max}$ (see above), we determined C_b for each value of C_T. From a curve fit analysis of ν/C_f vs ν (eq 3) values of $K_b = 2 \times 10^4$ M^{-1} and $n = 1.8$ and $K_b = 1 \times 10^5$ M^{-1} and $n = 3.0$ were obtained for the binding of CuCl$_2$ or Cu(CF$_3$SO$_3$)$_2$ to the Re(I) polymer respectively (see Figure 1).

Dynamic Light Scattering (DLS). *Poly-4-vinylpyridine (P4VP).* Dilute solutions of P4VP in dichloromethane (DCM) at concentrations between 0.2 and 0.5 mg mL^{-1} were analyzed at room temperature. The spectrum of the relaxation times L(ln τ) is a single peak centered at $\tau_0 = 39$ μs in all cases. The corresponding hydrodynamic radius R_h for the highest concentration is around 7.2 nm, as obtained from the Stokes−Einstein relation (see below). No significant changes were obtained from measurements at lower concentrations.

Re−P4VP Polymer. Solutions of Re−P4VP in acetonitrile at the same polymer concentration display a bimodal spectrum of relaxation times. Besides a short time peak centered at $\tau_{short} \sim 34$ μs, a very slow relaxation mode well separated from it was seen in all the data sets at $\tau_{long} \sim 0.72$ ms. Figure 2 shows a typical intensity weighted spectrum, where the maximum at the short-time mode represents one tenth of the contribution of the long-time mode.

Re−P4VP−CuCl$_2$ Polymer. A similar pattern is displayed by the solutions of Re−P4VP−CuCl$_2$ polymer. The two relaxation modes are centered at times $\tau_{short} \sim 29$ μs and $\tau_{long} \sim 0.46$ ms, respectively. Differences with the precedent system arise in the height and width of the short time contribution. In fact, the ratio of the amplitudes L(ln τ) at τ_{short} and τ_{long} is around 1.1, much higher than in the Re−P4VP polymer. The short-time peak also exhibits a noticeable broadening. Moreover, a closer inspection of the spectra shows a shift of the long-time peak toward smaller time values. These features are also shown in Figure 2, for the system analyzed at a polymer concentration 0.5 mg mL^{-1}. This pattern is similar for lower concentrations. Henceforth, we refer all our results to that polymer concentration.

Re−P4VP−Cu(CF$_3$SO$_3$)$_2$ Polymer. The time distribution spectra contain two peaks at 29 μs and 0.56 ms, with the short-time mode contributing around 50% of the long-time one. The broadening of the first peak is similar to that displayed by the Re−P4VP−CuCl$_2$ polymer system.

Static Light Scattering. The apparent radius of gyration of the solutes were estimated by measuring the time integrated light intensity at complementary scattering angles ($\theta = 45°$, 135°) and calculating the dissymmetry factor $Z_\theta = I_{exc}(\theta)/I_{exc}(\pi-\theta)$, where $I_{exc}(\theta)$ is the excess scattering of the solution ($= I_{solution}(\theta) - I_{solvent}(\theta)$). The results obtained for the systems Re−P4VP polymer, Re−P4VP−CuCl$_2$ polymer, and Re−P4VP−Cu(CF$_3$SO$_3$)$_2$ polymer were 5.2, 4.8, and 2.1, respectively. The high value of Z_{45} for the first two systems excludes the possibility of having rodlike or coiled structures and is only compatible with the elastic scattering from spherical objects. The last one allows the existence of coiled structures in addition.[37]

Solvent-Cast Films of the Polymers. The morphologies of the polymers Re−P4VP and Re−P4VP−CuCl$_2$ were studied by transmission electron microscopy (TEM). The polymer films were obtained by room temperature solvent evaporation of acetonitrile solutions of the Re−P4VP and Re−P4VP−CuCl$_2$ polymers, respectively. When taking photos, the polymer films were not stained with any chemicals, and the contrast of the image in the TEM photos can only originate from the rhenium complexes incorporated to the polymers. The Re(I) complexes in the polymer Re−P4VP aggregate and form isolated nanodomains that are dispersed in the polymer matrix film. The dimensions of the nanodomains are between 90 and 430 nm and are mainly spherical in shape. However, the polymer Re−

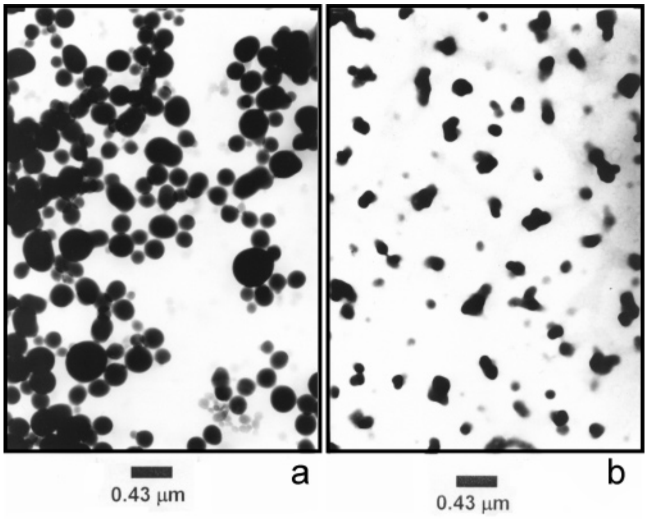

Figure 3. Transmission electron micrographs of the solvent cast films of the polymers (a) Re−P4VP and (b) Re−P4VP−$CuCl_2$.

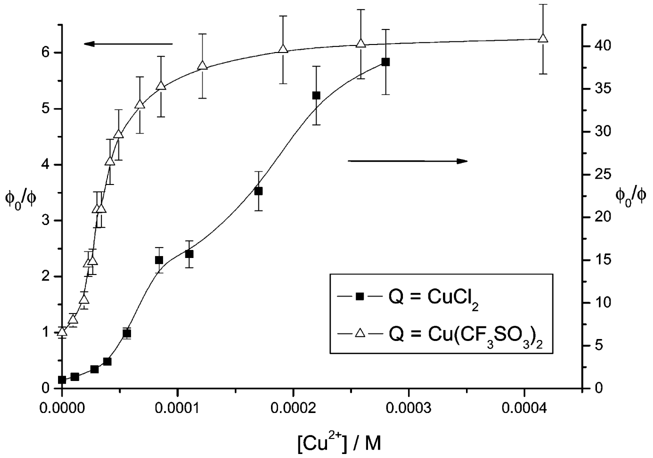

Figure 4. Steady-state quenching of $\{[(vpy)_2\text{-}vpyRe(CO)_3bpy]\ CF_3SO_3\}_{200}$'s luminescence by Cu(II) species: (■) Φ_0/Φ (right *y* axis), quencher = $CuCl_2$, (△) Φ_0/Φ (left *y* axis), quencher = $Cu(CF_3SO_3)_2$. See text for details.

P4VP−$CuCl_2$ aggregate to form nanodomains that are distorted from the spherical shape and whose dimensions are smaller than those nanodomains formed by the polymer Re−P4VP (see Figure 3). It should be noted that the dimensions of the two kinds of nanodomains are considerably larger than the full stretch length of the polymers. As a result, it is likely that the nanodomains contain a considerable number of polymer molecules.

Luminescence Quenching by Cu(II). The emission spectra of $CF_3SO_3[pyRe(CO)_3bpy]$ and Re−P4VP in deoxygenated CH_3CN at room temperature exhibited unstructured bands both centered at 589 nm with identical band shapes. The quenching of the luminescence of the Re(I) polymer by $CuCl_2$ and/or $Cu(CF_3SO_3)_2$ was studied using steady state and time-resolved techniques under similar experimental conditions ($[Re(I)] \sim 1 \times 10^{-4}$ M) to those utilized in the investigation of the binding of Cu(II) species to the Re(I) polyelectrolyte. As it can be observed from Figure 4, the quenching does not follow a Stern−Volmer kinetics. For instance, in the quenching by $Cu(CF_3SO_3)_2$, the ratio Φ_0/Φ follows a sigmoid curve with a limiting value of $(\Phi_0/\Phi)_{max} = 6.3$ at $[Cu(CF_3SO_3)_2] \sim 3 \times 10^{-4}$ M, which corresponds to 84% of the total emission quenched. Conversely, Φ_0/Φ in the quenching by $CuCl_2$ deviates upward with respect to the linear Stern−Volmer usual behavior with no limiting value of Φ_0/Φ. Moreover, at $[CuCl_2] \sim 3 \times 10^{-4}$ M, $\Phi_0/\Phi \sim 40$ (corresponding to 97% of the total emission quenched). Figure 5 shows the normalized emission spectra at different [Cu(II)] for the quenching by $CuCl_2$ (Figure 5a) and by $Cu(CF_3SO_3)_2$ (Figure 5b). As it can be observed from Figure 5a, the Re(I)-polymer emission spectra band shapes are not altered by $CuCl_2$ addition up to $[CuCl_2] < 6 \times 10^{-5}$ M. When the $[CuCl_2] > 8 \times 10^{-5}$ M there is a progressive shifting of the emission maximum from 589 to 555 nm. Figure 5b shows that there are hardly any changes in the normalized emission spectra of the Re(I)-polymer after the addition of $Cu(CF_3SO_3)_2$ in the same concentration range as with $CuCl_2$. However, the luminescence quenching of the monomer $CF_3SO_3[pyRe(CO)_3bpy]$ by CuX_2 (X = Cl or CF_3SO_3) follows a typical Stern−Volmer kinetics with $K_{sv,CuCl_2} = 4.6 \times 10^3$ M^{-1} and $K_{sv,Cu(CF_3SO_3)_2} = 2.1 \times 10^2$ M^{-1} respectively (see Figure 6). It is noteworthy that no spectral changes occur in the emission spectra of $CF_3SO_3[pyRe(CO)_3bpy]$ in the quenching of its luminescence by CuX_2 (X = Cl or CF_3SO_3).

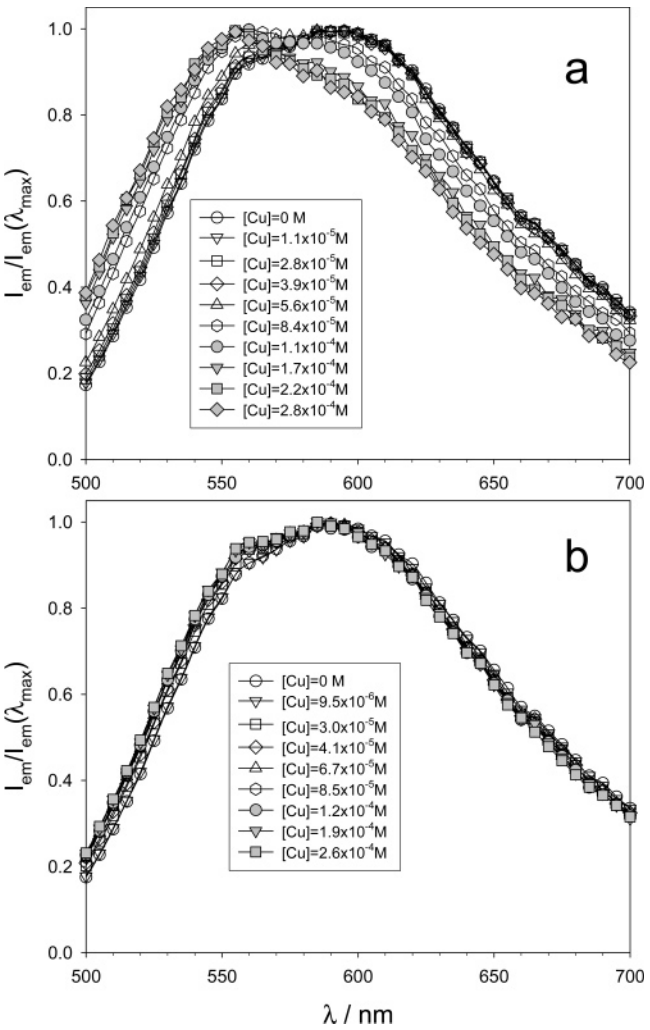

Figure 5. Normalized luminescence spectra of $\{[(vpy)_2\text{-}vpyRe(CO)_3bpy]\ CF_3SO_3\}_{200}$ at different Cu(II) concentrations in the quenching by (a) $CuCl_2$ and (b) $Cu(CF_3SO_3)_2$.

After excitation with a N_2 laser, the luminescence decay of the polymer Re−P4VP in acetonitrile is monoexponential with a lifetime of $\tau_{em} = 203$ ns.[28] However, after the addition of

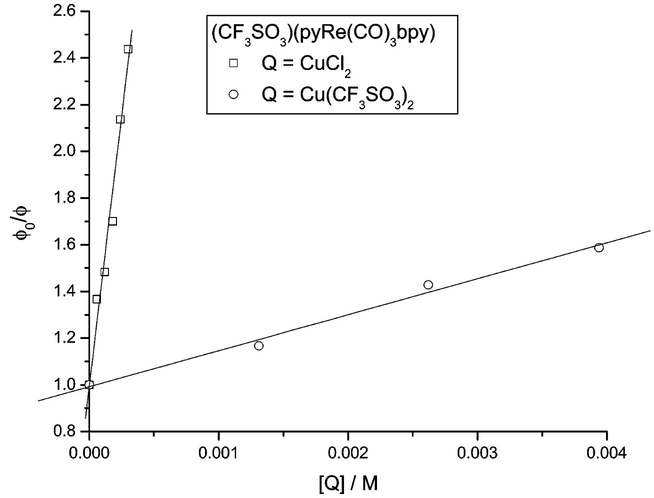

Figure 6. Stern−Volmer plots for the luminescence quenching of pyRe(CO)$_3$bpy$^+$ by (□) CuCl$_2$ and (○) Cu(CF$_3$SO$_3$)$_2$.

TABLE 1: Parameters Obtained in the Curve-Fit Analysis of the Experimental Luminescence Intensity, $I_{em}(t)$, According to a Biexponential Decay (Eq 4)[a]

[Cu(CF$_3$SO$_3$)$_2$]/ M	I_1/I_2	τ_1/ ns	τ_2/ ns	[CuCl$_2$]/ M	I_1/I_2	τ_1/ ns	τ_2/ ns
0		203[b]		0		203[b]	
9.8×10^{-6}		195[b]		1.2×10^{-5}		166[b]	
2.0×10^{-5}	1.47	190	44	2.4×10^{-5}	1.44	169	41
3.0×10^{-5}	0.63	148	34	3.6×10^{-5}	0.69	146	33
3.9×10^{-5}	0.39	126	30	4.8×10^{-5}	0.37	122	27
4.9×10^{-5}	0.29	119	29	6.0×10^{-5}	0.20	112	24
5.8×10^{-5}	0.27	114	27				
6.8×10^{-5}	0.25	116	27				
7.8×10^{-5}	0.21	131	27				
8.7×10^{-5}	0.17	131	27				

[a] See text for details. [b] Monoexponential decays.

CuX$_2$ (X = Cl or CF$_3$SO$_3$), the luminescence decay of the Re(I) polymer became biexponential, eq 4

$$I_{em}(t) = I_1 \exp(-t/\tau_1) + I_2 \exp(-t/\tau_2) \qquad (4)$$

Table 1 shows the values of the preexponential factors (I_1 and I_2) and the lifetimes (τ_1 and τ_2) obtained by a curve fit analysis of I_{em} according to eq 4 in the quenching of the luminescence of the Re(I)−polymer by CuX$_2$ (X = Cl and CF$_3$SO$_3$). Inspection of Table 1 shows that, as the Cu(CF$_3$SO$_3$)$_2$ concentration is increased, the ratio I_1/I_2 decreases. Besides, the longer lifetime τ_1 decreases from 203 ns (in the absence of quencher) to ~120 ns and eventually remains constant. The shorter lifetime also decreases from $\tau_2 \sim 40$ to 30 ns. At concentrations of Cu(CF$_3$SO$_3$)$_2$ $> 6 \times 10^{-5}$ M, both lifetimes τ_1 and τ_2 remain constant. A similar behavior is followed by the curve fit parameters I_1, I_2, τ_1, and τ_2 in the quenching by CuCl$_2$. Figure 7 shows a comparison of CuCl$_2$ and Cu(CF$_3$SO$_3$)$_2$ absorption spectra and the CF$_3$SO$_3$[pyRe(CO)$_3$bpy] luminescence spectrum.

Reductive Quenching by TEOA. The reductive quenching of the MLCT excited-state luminescence of the monomer CF$_3$SO$_3$[pyRe(CO)$_3$bpy] and polymer Re−P4VP by TEOA followed Stern−Volmer kinetics with K_{sv} values of 54 and 77 M^{-1} for the monomer and the polymer respectively (Figure 8).

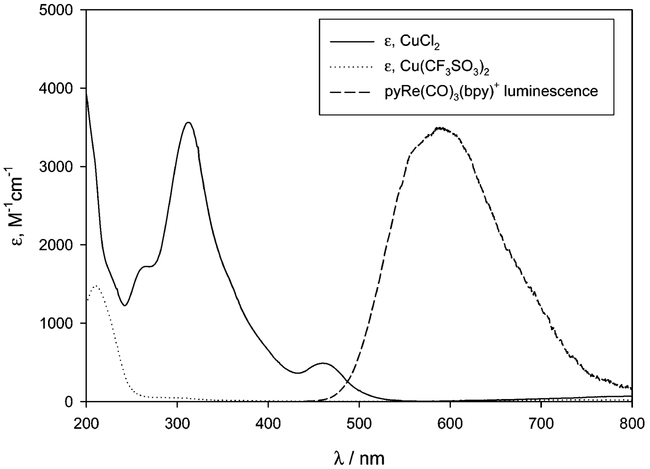

Figure 7. UV−vis absorption spectra of CuCl$_2$ and Cu(CF$_3$SO$_3$)$_2$. Comparison with pyRe(CO)$_3$bpy$^+$ luminescence spectrum.

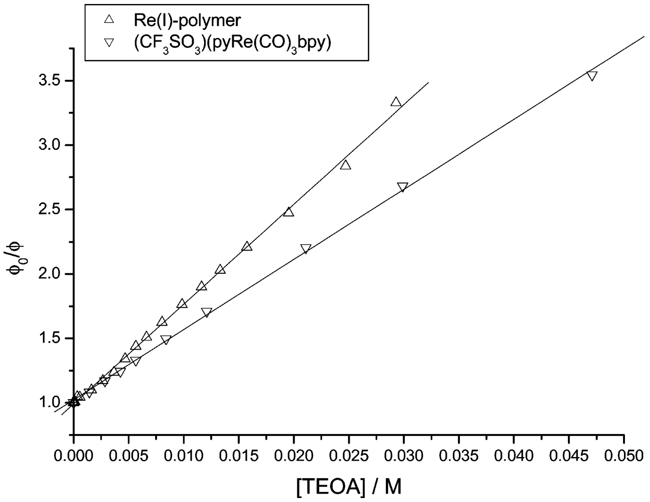

Figure 8. Stern Volmer plots for the luminescence quenching of {[(vpy)$_2$-vpyRe(CO)$_3$bpy] CF$_3$SO$_3$}$_{200}$ (polymer) and pyRe(CO)$_3$bpy$^+$ (monomer) by TEOA: (△) polymer's luminescence quenched by TEOA, (▽) monomer's luminescence quenched by TEOA.

Discussion

The coordination of CuCl$_2$ to poly-4-vinylpyridine (P4VP)[33] or to the partially methyl quaternized P4VP[32] has been reported in the literature. The new absorption bands generated after the coordination of CuX$_2$ to the Re−P4VP polymer have λ_{max} = 725 and 610 nm when X = Cl and CF$_3$SO$_3$, respectively. These facts can be compared with the similar shift of the absorption maximum from 770 to 610 nm and an increase of the molar extinction coefficient observed in the stepwise formation of CuL$_i^{2+}$ complexes, (i = 1−4) with L = ethylpyridine,[32] in water as a solvent. This is because the pyridine produces a stronger ligand field, which causes the absorption band to move from the far red to the middle of the red region of the spectrum. Besides, an increase in the d−d extinction coefficient after coordination of pyridine to Cu(II) should be related to a decrease in the symmetry around the metal center. It is reasonable to assume then that the complexation of CuCl$_2$ to the Re−P4VP polymer to form the polymer Re−P4VP−CuCl$_2$ proceeds with a lower average coordination number than in the complexation of Cu(CF$_3$SO$_3$)$_2$ to the Re(I) polymer to form the polymer Re−P4VP−Cu(CF$_3$SO$_3$)$_2$. Indeed, approximate coordination numbers being 2 and 3 were calculated from UV−vis changes for CuCl$_2$ and Cu(CF$_3$SO$_3$)$_2$ respectively (see above).

The single peak in the P4VP/DCM spectrum at 39 μs is the fingerprint of the translational diffusion behavior of the single polymer molecules in dilute solutions. The Stokes−Einstein

TABLE 2: Relaxation Times τ_1 and τ_2 (in Milliseconds), Relative Contributions, and Hydrodynamic Radii R_1 and R_2 (in Nanometers) at the Peaks of the Corresponding Distributions[a]

system	τ_1/ms	$L(\ln \tau_1)$	τ_2/ms	$L(\ln \tau_2)$	R_1/nm	R_2/nm
P4VP	0.039 (0.005)	1.00			7.2 (0.6)	
Re−P4VP	0.034 (0.005)	0.10	0.72 (0.03)	1.0	7.4 (1.0)	156 (6)
Re−P4VP−$CuCl_2$	0.029 (0.004)	1.0	0.46 (0.06)	0.90	6.2 (0.8)	96 (11)
Re−P4VP−$Cu(CF_3SO_3)_2$	0.029 (0.003)	0.50	0.56 (0.03)	1.0	6.9 (0.7)	137 (8)

[a] Here, the label 1 (2) replaces the name "short" ("long") used in the text. Figures in parentheses represent standard deviations.

equation relates the hydrodynamics radius of the polymer R_h with the relaxation time τ

$$R_h = k_B T q^2 \tau / 6\pi\eta \tag{5}$$

where k_B is the Boltzmann constant, T is the absolute temperature, and η is the shear viscosity of the solvent in the dilute solution regime. The maximum of the unweighted radius distribution is at $R_h = 7.2 \pm 0.6$ nm. Here and below we report the mean value of relaxation times and radii at the maxima of the corresponding distributions and the standard deviation of the mean, from the statistics of at least 10 independent experiments. The literature value of the unperturbed radius of gyration R_G of monodisperse P4VP with a molecular weight 6×10^4 g mol^{-1}(which corresponds to the M_w of P4VP polymer used in the preparation of Re−P4VP polymer[26]) in solvents such as water and ethanol at 25 °C is 7.1 nm.[37] Hence, we find a good agreement between the polymer size determined from DLS and published data in other solvents. Exact determination of the radius of gyration was out of the scope of this work and will be reported elsewhere.

The bimodal relaxation time spectra registered in the systems Re−P4VP polymer, Re−P4VP−$CuCl_2$ polymer and Re−P4VP−$Cu(CF_3SO_3)_2$ polymer reveals the existence of bigger structures with diffusion times $\tau_{\mathrm{long}} > 10\ \tau_{\mathrm{short}}$ coexisting with smaller ones associated to τ_{short}. In fact, these latter structures are identified as Re−P4VP macromolecules in the scale of 6−8 nm say, of the same size as that of P4VP in DCM. Since the molecular weight of Re−P4VP polymers is around 1.8×10^5 g mol $^{-1}$, it appears that these polymers would adopt in acetonitrile more compact conformations than their parents P4VP in DCM.

On the other hand, the mean size of the bigger micelles can be obtained from the value of the relaxation time at the corresponding maximum of the distribution $L(\ln \tau_{\mathrm{long}})$ assuming the same hydrodynamic model. We note that the wide distribution of relaxation times between τ_{short} and τ_{long} implies a wide distribution of sizes of spherical objects, ranging from a few nanometers at polymer scales to few hundreds of nanometers covering micelle scales.

In Table 2, we reproduce mean values and standard deviations of the mean of relaxation times and hydrodynamic radius at the peaks of the time and radius distributions for the three systems Re−P4VP polymer, Re−P4VP−$CuCl_2$ polymer, and Re−P4VP−$Cu(CF_3SO_3)_2$ polymer. The system P4VP/DCM was also included for comparison.

Average polymer sizes are not modified by the incorporation of CuX_2 to Re−P4VP, but significant changes are evident in the size of the companying micelles. The reduction in size of the Re−P4VP−CuX_2 micelles is more important for Re−P4VP−$CuCl_2$ than Re−P4VP−$Cu(CF_3SO_3)_2$.

The size distributions are similar to time distributions, shifted by the factor given by eq 5. We note that the shape of the three distributions at micelles scales are the same, only a shift to lower sizes (times) is evident. Instead, the distributions of the systems with Cu(II) compounds at polymer scales broaden and increase in height, demonstrating an increase of the relative "population" of Re−P4VP−CuX_2 polymers with respect to that of the corresponding micelles.

The radii of gyration revealed by SLS measurements were obtained assuming spherical solutes using tabulated values of their scattering form factor.[37] We obtained 91, 89, and 67 nm for the three Re−P4VP polymer, Re−P4VP−$CuCl_2$ polymer, and Re−P4VP−$Cu(CF_3SO_3)_2$ polymer, respectively. If a coiled structure is assumed for the latter system, the corresponding radius of gyration would be a little higher, between 76 and 80 nm depending on the (unknown) polydispersity of the sample.

Clearly, these figures correspond to some weighted average of the coexisting structures detected by DLS. Size differences of the three systems are less noticeable here, but they are consistent with the picture provided by DLS, i.e., two independent structures at equilibrium, polymer and micelles, with relative compositions depending on the particular system.

Assuming that the mean density of a given micelle is the same as that of an isolated Re−P4VP random coil polymer and neglecting solvation contributions to R_h, a ratio

$$\frac{M_w(\mathrm{micelle})}{M_w(\mathrm{polymer})} \approx \left(\frac{R_2}{R_1}\right)^2 \tag{6}$$

can roughly be estimated giving 4.4×10^2, 3.9×10^2, and 2.4×10^2 for Re−P4VP, Re−P4VP−$Cu(CF_3SO_3)_2$, and Re−P4VP−$CuCl_2$ polymers, respectively. Those figures represent, roughly speaking, the number of single polymers that could aggregate to form the micelles.

TEM images obtained for Re−P4VP and Re−P4VP−$CuCl_2$ polymers are in good agreement with the calculated $R_2 = 156 \pm 6$ nm and $R_2 = 96 \pm 11$ nm from DLS experiments for the micelles of the Re−P4VP and Re−P4VP−$CuCl_2$ polymers, respectively. The ratio $L(\ln \tau_1)/L(\ln \tau_2)$ is 0.1, 1.1, and 0.5 for the Re−P4VP, Re−P4VP−$CuCl_2$, and Re−P4VP−$Cu(CF_3SO_3)_2$ polymers, respectively. This fact suggests that coordination of Cu(II) to Re−P4VP breaks the original micelle reducing its radius and increasing the number of polymers that are not forming micelles. This effect is more important (both in augmenting $L(\ln \tau_1)/L(\ln \tau_2)$ and reducing R_2) when the copper salt used was $CuCl_2$ than $Cu(CF_3SO_3)_2$. TEM images show that the reduction of the micelle radius is accompanied by a distortion from the spherical shape toward some elongated structure. The short-time peak for Re−P4VP−$CuCl_2$ and Re−P4VP−$Cu(CF_3SO_3)_2$ polymers in Figure 2 also exhibits a noticeable broadening when compared to the one for Re−P4VP polymer. This means that after coordinating by Cu(II) to the free pyridines the resulting Re(I)-P4VP−Cu(II) polymers that are now not forming micelles may show a huge variety of structures (and a concomitant broadening of the distribution around R_1) since intramolecular coordination between adjacent vpy units on the polymer chain is not possible in P4VP[33] and all P4VP complexes should be perforce cross linked by Cu(II). The distortion of the

SCHEME 2

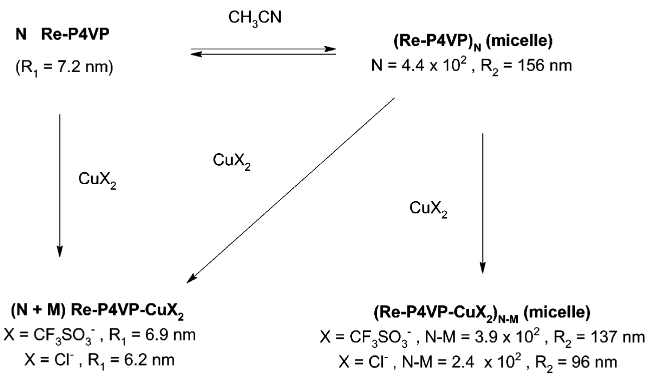

Re−P4VP micelles in the presence of $CuCl_2$ as shown by TEM is also supporting the existence of cross linked Re−P4VP polymers by Cu(II). Because $CF_3SO_3^-$ is a weak ligand, it can explain the apparent higher coordination number. Indeed, $CF_3SO_3^-$ is a poor ligand (compared to Cl^-), and it does not compete with pyridine ligands.[28] In fact, in $Cu(CF_3SO_3)_2$ acetonitrile solutions, the predominant species should be $Cu(CH_3CN)_4^{+2}$; however, in $CuCl_2$ acetonitrile solutions, a significant presence of other species should be considered. Binding constants of $K_b = 2 \times 10^4$ M^{-1} and 1×10^5 M^{-1} were calculated for the interaction of Re−P4VP polymer with $CuCl_2$ and Cu $(CF_3SO_3)_2$, respectively. Probably, the lower value of K_b in the case of $CuCl_2$ is due to the Cl^- in the sphere of coordination of Cu(II). On the other hand, the 10−100 fold lower values for K_b reported in the literature for the interaction of partially methyl quaternized P4VP with $Cu(NO_3)_2$ in aqueous solutions[32] may be explained by a reduction of the pyridine basicity due to protonation of the pyridinic nitrogen in water solutions. Scheme 2 depicts the distribution of species that may be encountered in solution after the binding of Cu(II) to the Re−P4VP polymer. Our experiments show that after excitation with a N_2 laser the luminescence decay of the polymer Re−P4VP in acetonitrile is monoexponential, $\tau_{em} = 203$ ns. It is so although the Re−P4VP polymer molecules are aggregated forming micelles in acetonitrile. We do not have experimental evidence about the structures of those micelles. However, some speculations can be made. For instance, P4VP is nearly insoluble in acetonitrile, but this solvent is a good one for the Re−P4VP polymer. Then it is plausible to imagine that the inner core of the micelles will be formed mainly by the free pyridines of the Re−P4VP polymers and the outer part will be constituted mainly by the Re(I) chromophores. The observation of a monoexponential decay of the MLCT luminescence means that the majority of these chromophores are in approximately equivalent environments on the surface of the micelles. However, a second-order process was observed in addition to the first-order decay of the Re−P4VP MLCT luminescence when the sample was excited by higher power laser sources, such as Nd:YAG (355 nm) and XeF (351 nm) excimer lasers.[28] The second-order processes observed in the MLCT luminescence decay of the Re−P4VP polymer could be a consequence of the production of a high number of MLCT excited states in close proximity in the micelles due to the intense Nd:YAG (355 nm) and XeF (351 nm) laser pulses. In these conditions, excited-state self-annihilation can occur.

The quenching of the Re−P4VP polymer's luminescence by CuX_2 (X = Cl or CF_3SO_3) proceeds via both dynamic and static mechanisms as it can be observed from the comparison of Φ_0/Φ (Figure 4) and τ functional dependences (Table 1) on Cu(II) concentration. For instance, in the luminescence (steady state or time resolved) quenching by $Cu(CF_3SO_3)_2$, we have [Re(I)] $\sim 1 \times 10^{-4}$ M and $[py]_{uncoordinated} \sim 2 \times 10^{-4}$ M and hence $C_{b,max} \sim 7 \times 10^{-5}$ M. From Table 1, it can be observed that at $[Cu(CF_3SO_3)_2] \sim 7 \times 10^{-5}$ M both lifetimes τ_1 and τ_2 achieve constant values. However, Figure 4 shows that the quenching measured by steady-state luminescence techniques (increase in the ratio Φ_0/Φ vs Cu(II) concentration) is still significant at $[Cu(CF_3SO_3)_2] > 7 \times 10^{-5}$ M. A limiting plateau in Φ_0/Φ is achieved only at $[Cu(CF_3SO_3)_2] > 1.5 \times 10^{-4}$ M. Moreover, results from steady-state experiments (Figure 5a) with $CuCl_2$ must be associated too with more than one quenching process. For instance, when $0 < [CuCl_2] < C_{b,max} \sim 7 \times 10^{-5}$ M, the quenching proceeds with no spectral changes in the luminescence spectra. However, when $[CuCl_2] > C_{b,max}$ there is a progressive shifting of the emission maximum to shorter wavelengths. This behavior could be attributed to some kind of interaction between $CuCl_X^{(2-x)}$ species and the Re(I)−polymer. This effect was not observed in the quenching by $Cu(CF_3SO_3)_2$ (compare panels a and b of Figure 5). On the other hand, the monomer $CF_3SO_3[pyRe(CO)_3bpy]$ luminescence is quenched by $CuCl_2$ and by $Cu(CF_3SO_3)_2$ following typical Stern−Volmer kinetics with no spectral changes in the luminescence spectrum even at higher [Cu(II)] than those used when quenching the luminescence of the Re−P4VP polymer.

The luminescence quenching by $Cu(CF_3SO_3)_2$ in the Re(I) polymer is far more efficient than in the monomer (compare Figures 4 and 6). There are two different reasons that can explain such a difference. First, there should be an enhancement of the energy transfer rate constant due to a close vicinity between the Re(I) chromophore and the Cu(II) bound to a near pyridine in the polymer. Second, an enhancement of the spectral overlap integral (J) between the emission spectrum of the Re(I) chromophore and the new absorption band which appears after the coordination of the Cu(II) ion to the Re−P4VP polymer (note that the Dexter's exchange mechanism for energy transfer predicts that $k_{et} \alpha \exp(-R)$, whereas the Forster's dipole-induced energy transfer theory predicts that $k_{et} \alpha R^{-6}$; that is, both theories predict an increase of k_{et} as R decreases. Besides, in both Dexter's and Forter's theories $k_{et} \alpha J$).[40] The quenching of the monomer $CF_3SO_3[pyRe(CO)_3bpy]$ luminescence by $CuCl_2$ follows a typical Stern−Volmer kinetics and taking into account its luminescence lifetime[28] a bimolecular rate constant $k_{q,CuCl_2} = 2 \times 10^{10}$ M^{-1} s^{-1} can be calculated, the value of which is close to the diffusional limit in acetonitrile.[41] A far lower bimolecular rate constant $k_{q,Cu(CF_3SO_3)_2} = 8 \times 10^8$ M^{-1} s^{-1} can be calculated from the quenching by $Cu(CF_3SO_3)_2$ (Figure 6). The poor spectral overlap integral (J) between the absorption spectrum of $Cu(CF_3SO_3)_2$ and the $CF_3SO_3[pyRe(CO)_3bpy]$ emission spectrum (see Figure 7) should be responsible for this distinct photophysical behavior.

The binding of Cu(II) to the Re(I) polymer produces the breakage of the micelles and yields a wide distribution of particle sizes ranging from a few nanometers at polymer scales to a few hundreds of nanometers covering micelle scales. In fitting the luminescence decay by a biexponential function, the parameters τ_1 and τ_2 may then be viewed as "mean" lifetimes representing average contributions from the different species.

The reductive quenching of the $\{[(vpy)_2\text{-}vpyRe(CO)_3bpy]CF_3SO_3\}_{200}$ and $CF_3SO_3[pyRe(CO)_3bpy]$ MLCT excited states by TEOA[26,41] are represented in eqs 7−10

$$[(\mathrm{vpy})_2\text{-vpyRe}^{(+)}(\mathrm{CO})_3\mathrm{bpy}]_{m+n} \xrightarrow{h\nu} [(\mathrm{vpy})_2\text{-vpyRe}^{(+)}(\mathrm{CO})_3\text{-}\mathrm{bpy(GS)}]_n[(\mathrm{vpy})_2\text{-vpyRe}^{(2+)}(\mathrm{CO})_3(\mathrm{bpy}^-)(\mathrm{MLCT})]_m \quad (7)$$

$$[(\mathrm{vpy})_2\text{-vpyRe}^{(+)}(\mathrm{CO})_3\mathrm{bpy(GS)}]_n[(\mathrm{vpy})_2\text{-vpyRe}^{(2+)}(\mathrm{CO})_3(\mathrm{bpy}^-)(\mathrm{MLCT})]_m + m\mathrm{TEOA} \rightarrow [(\mathrm{vpy})_2\text{-vpyRe}^{(+)}(\mathrm{CO})_3\mathrm{bpy(GS)}]_n[(\mathrm{vpy})_2\text{-vpyRe}^{(+)}(\mathrm{CO})_3(\mathrm{bpy}^-)]_m + m\mathrm{TEOA}^+ \quad (8)$$

$$\mathrm{pyRe}^{(+)}(\mathrm{CO})_3(\mathrm{bpy})(\mathrm{GS}) \xrightarrow{h\nu} \mathrm{pyRe}^{(2+)}(\mathrm{CO})_3(\mathrm{bpy}^-)(\mathrm{MLCT}) \quad (9)$$

$$\mathrm{pyRe}^{(2+)}(\mathrm{CO})_3(\mathrm{bpy}^-)(\mathrm{MLCT}) + \mathrm{TEOA} \rightarrow \mathrm{pyRe}^{(+)}(\mathrm{CO})_3(\mathrm{bpy}^-) + \mathrm{TEOA}^+ \quad (10)$$

where $m + n = 200$ in the polymer, $-\mathrm{vpyRe}^{(2+)}(\mathrm{CO})_3(\mathrm{bpy}^-)$ stands for the MLCT(Re → bpy) excited state, and $-\mathrm{vpyRe}^{(+)}(\mathrm{CO})_3(\mathrm{bpy}^-)$ is the reduced radical produced after the reductive quenching by the sacrificial reductant TEOA, eq 8.

The Re−P4VP polymer's luminescence reductive quenching by TEOA follows a typical Stern−Volmer kinetics (see Figure 8). From the Stern−Volmer constant $K_{\mathrm{sv}} = 77\ \mathrm{M}^{-1}$ and the luminescence lifetime[28] in acetonitrile, a bimolecular quenching constant $k_{\mathrm{q}} = 3.8 \times 10^8\ \mathrm{M}^{-1}\ \mathrm{s}^{-1}$ can be calculated. The quenching of the monomer $\mathrm{CF_3SO_3[pyRe(CO)_3bpy]}$ luminescence by TEOA also follows a Stern−Volmer kinetics with a lower $K_{\mathrm{sv}} = 54\ \mathrm{M}^{-1}$. Taking into account its luminescence lifetime, a bimolecular quenching constant $k_{\mathrm{q}} = 2.2 \times 10^8\ \mathrm{M}^{-1}\ \mathrm{s}^{-1}$ can be calculated.

According to Marcus, the outer sphere reorganization energy depends on the size of reactants and the separation distance, as well as on the dielectric properties of the embedding solvent. The theory, in its original formulation, was developed for a homogeneous solution. Thus, to describe the electron transfer data on micelle surfaces, we should properly account for the heterogeneous local structure of micelles. However, Marcus theory of electron transfer has already been extended to micelles.[42] In this regards, micelles are supposed to provide a good reaction media to observe the Marcus inverted region for bimolecular electron-transfer reactions. In fact, the Marcus inverted region has been observed in electron-transfer reactions between coumarin dyes and amines in micellar solution.[43] Because of the rigid structures of the micelles, reactants will be entangled within the micellar chains and thus their movements will be highly restricted. In other words, the high viscosity of the micellar media prevents the diffusion of the reactants, and if the electron transfer reactions are relatively faster than diffusion, then the bimolecular reactions in micellar solutions can be envisaged as the effective intramolecular reactions. Thus, the reaction dynamics in the micellar media is expected to differ largely as compared to that in the homogeneous media.

Taking into account the oxidation redox potential of TEOA,[41] the reduction potential of the complex $\mathrm{pyRe(CO)_3bpy^+}$,[44] and the energy of the excited state which can be estimated from the emission spectrum as $E_{0-0} \sim 2.37$ eV, we can calculate a $\Delta G \sim -0.4$ eV for the forward electron-transfer reaction between $\mathrm{pyRe(CO)_3bpy^+}$'s MLCT excited state and TEOA. The polymer should have a similar ΔG value. This ΔG value lies in the Marcus normal region.[41] It is well-known that the motion of the solvent molecules in the restricted media, i.e., in micelles, is retarded by several orders of magnitude compared to that in homogeneous solvents. Thus, the solvent reorganization may not contribute completely within the time scale of the electron-transfer reaction between the Re(I)−polymer's MLCT and TEOA. The fact that the polymer's k_{q} is nearly 2 times higher than that of the monomer may be reflecting a contribution from the polymer backbone to a decrease of the Marcus inner sphere reorganization energy (λ_i) of the electron-transfer process via vibrational modes of the uncomplexed pyridines in the polymer backbone. However, a higher value of k_{q} in the polymer than in the monomer may also be explained due to the fact that the diffusion of the TEOA molecules to form the encounter complex with the Re(I) chromophore is favored-compared to the monomer, due to the fact that TEOA might have a tendency to be close to the polymer by hydrogen bonding interactions with the free pyridine groups and may thus more often encounter Re(I) chromophores than in the case for the monomer $\mathrm{pyRe(CO)_3bpy^+}$.

Concluding Remarks

TEM images and DLS experiments have demonstrated that Re−P4VP polymers aggregate to form mainly spherical micelles whose dimensions are in the range of 90−430 nm. After the coordination of Cu(II) species to the Re(I) polymer, the polymer Re−P4VP−$\mathrm{CuCl_2}$ aggregates to form micelles that are distorted from the spherical shape and whose dimensions are smaller than those micelles formed by the polymer Re−P4VP.

The coordination of Cu(II) species to the polymer $\{[(\mathrm{vpy})_2\text{-vpyRe(CO)}_3\mathrm{bpy}]\ \mathrm{CF_3SO_3}\}_{200}$ produces the quenching of the MLCT excited state by energy transfer processes that are more efficient than those in the quenching of the monomer's luminescence by Cu(II). Besides, the kinetics of the quenching by Cu(II) does not follow a Stern−Volmer behavior. Moreover, although in the quenching of the polymer $\{[(\mathrm{vpy})_2\text{-vpyRe(CO)}_3\mathrm{bpy}]\ \mathrm{CF_3SO_3}\}_{200}$ luminescence by $\mathrm{Cu(CF_3SO_3)_2}$ the ratio Φ_0/Φ shows a sigmoid dependence on $\mathrm{Cu(CF_3SO_3)_2}$ concentration with a limiting value of $\Phi_0/\Phi \sim 6$, the quenching by $\mathrm{CuCl_2}$ does not show a plateau on Φ_0/Φ. Conversely, the reductive redox quenching of the Re(I) polymer's MLCT excited state by TEOA follows a Stern−Volmer kinetics. The striking differences found in the quenching mechanisms with Cu(II) or TEOA are a consequence of the strong chemical interaction (binding) of Cu(II) to the poly-4-vynilpyridine backbone of the Re(I)−polymer. All of the quenching processes either by Cu(II) or TEOA are more efficient in the polymer than in the monomer.

Acknowledgment. This work was supported in part by a project grant from Agencia de Promoción Científica y Tecnológica de Argentina (ANPCyT Grant No. PICT 06-12610), Consejo Nacional de Investigaciones Cientificas y Tecnológicas (CONICET-PIP 02470/00), Universidad Nacional de La Plata, and the Comisión de Investigaciones Científicas de la Provincia de Buenos Aires (CICPBA). E.W. thanks CONICET for a personal research grant.

References and Notes

(1) Stufkens, D. J. *Comments Inorg. Chem.* **1992**, *13*, 359.
(2) Stor, G. J.; Stufkens, D. J.; Oskam, A. *Inorg. Chem.* **1992**, *31*, 1318.
(3) Rossenaar, B. D.; Stufkens, D. J.; Vlček, A., Jr. *Inorg. Chem.* **1996**, *35*, 2902.
(4) Liard, D. J.; Vlček, A., Jr. *Inorg. Chem.* **2000**, *39*, 485.
(5) Wolcan, E.; Torchia, G.; Tocho, J.; Piro, O.; Juliarena, P.; Ruiz, G.; Féliz, M. R. *J. Chem. Soc. Dalton Trans.* **2002**, *10*, 2194.
(6) Fox, M. A., Chanon, M., Eds.; *Photoinduced Electron Transfer*; Elsevier: Amsterdam, 1988.
(7) Balzani, V.; Bolleta, F.; Gandolfi, M. T.; Maestri, M. *Top. Curr. Chem.* **1978**, *75*, 1.
(8) Grätzel, M., Ed.; *Energy Resources Through Photochemistry and Catalysis*; Academic Press: New York, 1983.
(9) Kalyanasundaram, K. *Coord. Chem. Rev.* **1982**, *46*, 159.

(10) Kalyanasundaram, K., Grätzel, M., Eds.; *Photosensitization and Photocatalysis Using Inorganic and Organometallic Compounds*; Kluwer Academic Publishers: Norwell, MA, 1993.

(11) Chen, L. X.; Jäger, W. J. H.; Gosztola, D. J.; Niemczyk, M. P.; Wasielewski, M. R. *J. Phys. Chem. B* **2000**, *104*, 1950.

(12) Wang, B.; Wasielewski, M. R. *J. Am. Chem. Soc.* **1997**, *119*, 12.

(13) Wang, Q.; Wang, L.; Yu, L. *J. Am. Chem. Soc.* **1998**, *120*, 12860.

(14) Olmsted, J., III.; McClanahan, S. F.; Danielson, E.; Younathan, J. N.; Meyer, T. J. *J. Am. Chem. Soc.* **1987**, *109*, 3297.

(15) Younathan, J. N.; McClanahan, S. F.; Meyer, T. J. *Macromolecules* **1989**, *22*, 1048.

(16) Worl, L. A.; Strouse, G. F.; Younathan, J. N.; Baxter, S. M.; Meyer, T. J. *J. Am. Chem. Soc.* **1990**, *112*, 7571.

(17) Baxter, S. M.; Jones, W. E., Jr.; Danielson, E.; Worl, L. A.; Strouse, G. F.; Younathan, J. N.; Meyer, T. J. *Coord. Chem. Rev.* **1991**, *111*, 47.

(18) Jones, W. E., Jr.; Baxter, S. M.; Strouse, G. F.; Meyer, T. J. *J. Am. Chem. Soc.* **1993**, *115*, 7363.

(19) Dupray, L. M.; Meyer, T. J. *Inorg. Chem*. **1996**, *35*, 6299.

(20) Suzuki, M.; Kimura, M.; Hanabusa, K.; Shirai, H. *J. Chem. Soc., Faraday Trans.* **1997**, *93*, 4137.

(21) Dupray, L. M.; Devenney, M.; Striplin, D. R.; Meyer, T. J. *J. Am. Chem. Soc.* **1997**, *119*, 10243.

(22) Friesen, D. A.; Kajita, T.; Danielson, E.; Meyer, T. J. *Inorg. Chem.* **1998**, *37*, 2756.

(23) Worl, L. A.; Jones, W. E., Jr.; Strouse, G. F.; Younathan, J. N.; Danielson, E.; Maxwell, K. A.; Sykora, M.; Meyer, T. J. *Inorg. Chem.* **1999**, *38*, 2705.

(24) Smith, G. D.; Maxwell, K. A.; DeSimone, J. M.; Meyer, T. J.; Palmer, R. A. *Inorg. Chem.* **2000**, *39*, 893.

(25) Connors, Jr. P. J.; Tzalis, D.; Dunnick, A. L.; Tor, Y. *Inorg. Chem*. **1998**, *37*, 1121.

(26) Wolcan, E.; Ferraudi, G. *J. Phys. Chem. A* **2000**, *104*, 9281.

(27) Walters, K. A.; Ley, K. D.; Cavalaheiro, C. S. P.; Miller, S. E.; Gosztola, D.; Wasielewski, M. R.; Bussandri, A. P.; van Willigen, H.; Schanze, K. S. *J. Am. Chem. Soc.* **2001**, *123*, 8329.

(28) Wolcan, E.; Feliz, M. R. *Photochem. Photobiol. Sci.* **2003**, *2*, 412.

(29) Hou, S.; Chan, W. K. *Macromol. Rapid Commun.* **1999**, *20*, 440.

(30) Hou, S.; Man, K. Y. K.; Chan, W. K. *Langmuir* **2003**, *19*, 2485.

(31) Tsuchida, E.; Kaneko, M.; Nishide, H. *Makromol. Chem.* **1973**, *164*, 203.

(32) Kirsh, Y. E.; Kovner, V. Ya.; Kokorin, A. I.; Zamaraev, K. I.; Cherniak, V. Ya.; Kabanov, V. A. *Eur. Polym. J.* **1974**, *10*, 671.

(33) Agnew, H. *J. Polym. Sci.* **1976**, *14*, 2819.

(34) Nishide, H.; Tsuchida, E. *J. Polym. Sci.* **1981**, *19*, 835.

(35) Jeschke, G. *J. Phys. Chem. B* **2000**, *104*, 8382.

(36) Provencher, S. W. *Comput. Phys. Commun.* **1982**, *27*, 213.

(37) Brandrup, J., Immergut, E. H., Eds.; *Polymer Handbook, 3rd ed.*; Wiley: New York, 1989; VII/39; VII/485.

(38) Scatchard, G. *Ann. N.Y. Acad. Sci.* **1949**, *51*, 660.

(39) McGhee, J. D.; von Hippel, P. H. *J. Mol. Biol.* **1974**, *86*, 469.

(40) Turro, N. J. *Modern Molecular Photochemistry*; University Science Books: Mill Valley, CA, 1991; Chapter 9.

(41) Ruiz, G.; Rodriguez-Nieto, F.; Wolcan, E.; Féliz, M. R. *J. Photochem. Photobiol. A: Chem.* **1997**, *107*, 47.

(42) Tavernier, H. L.; Barzykin, A. V.; Tachiya, M.; Fayer, M. D. *J. Phys. Chem. B* **1998**, *102*, 6078.

(43) Kumbhakar, M.; Nath, S.; Mukherjee, T.; Pal, H. *J. Chem. Phys.* **2004**, *120*, 2824.

(44) Sacksteder, L. A.; Zipp, A. P.; Brown, E. A.; Streich, J.; Demas, J. N.; DeGraff, B. A. *Inorg. Chem.* **1990**, *29*, 4335.